Daytime Optical Contributions Toward Timely Space Domain Awareness in Low Earth Orbit

Jeff Shaddix*
Numerica Corporation
Cameron Key, Alex Ferris, James Herring, Navraj Singh, Todd Brost, Jeff Aristoff
Numerica Corporation, 5042 Technology Parkway, Suite 100, Fort Collins, CO 80528

ABSTRACT

As object density in Low Earth Orbit (LEO) continues to increase, so increases the need for time-critical space domain awareness (SDA) information on select objects of interest. While radar systems provide the bulk of LEO tracking data, their overall cost per sensor prohibits widespread proliferation and leads to temporal coverage gaps that can hinder decision making. In this paper, we investigate how a hypothetical network of low-cost cathemeral (active throughout day and night) optical telescope systems can supplement radar systems for enhanced custody of any given subset of detectable LEO objects. We perform sensor access and data quality simulations accounting for weather, solar exclusion, capacity, and accuracy limitations to present salient performance statistics such as time delays since last observation and position knowledge error. We conclude that, despite certain limitations, cathemeral optical systems can provide an inexpensive and effective approach to enhancing timely LEO SDA.

1. INTRODUCTION

The low Earth orbit (LEO) satellite population is burgeoning. Commercial, academic, and government programs continue to see proliferated LEO constellations as a key to success, which both necessitates and complicates timely space domain awareness (SDA). As the LEO population grows, so do situations that pose risk to spacecraft (unmanned or manned) and the relevant missions that led them there. Some examples include rendezvous and proximity operations (RPOs), conjunctions/collisions, orbital insertions, reentries, and orbital proximity to maneuverable and/or separable satellites. These situations may warrant timely SDA with high revisit rates on a subset of the LEO resident space object (RSO) population at any given time.

Radar systems are predominantly responsible for maintaining a complete and up-to-date catalog of RSOs in LEO. However, these systems are costly to build and maintain which naturally limits the number of sites in operation around the world. Consequently, revisit rates, i.e., the time between successive observations of the same satellite, may be too low to support certain time-critical SDA-related situations such as those mentioned above.

Optical systems are often used to track RSOs in geosynchronous Earth orbit (GEO) and other deep space regimes, but when properly-equipped they can also track RSOs in LEO. The necessary equipment generally consists of gimbals with accurate tracking/reporting at angular velocities of at least 1 degree/sec and a high-accuracy timing solution for gimbal control and exposure time-tagging. Optical systems take measurements in angle-only space, compared to radar, which measure range and potentially range-rate. Furthermore, many payloads and rocket bodies in LEO are large enough to easily be seen by smaller optical apertures. That said, there is a natural trade-off between detectability and field-of-view (FOV), especially in areas of light pollution or on moonlit nights. In order to maximize detectability, a telescope will typically "rate track" by keeping the RSO stationary in the camera frame – tracking only one RSO at a time or multiple in close formation. Finally, ground-based optical can be hampered by cloud cover; consequently, multiple sites are often used to provide mitigation with geographic diversity. Regardless, given optical systems are a relatively cheap alternative to radar installations, it would seem optical systems are well-suited for proliferation to serve time-critical SDA scenarios, but there is another issue to explore.

Traditional ground-based optical telescopes are "nocturnal" (henceforth dubbed nocturnal telescopes) in the sense that they can only operate at night. Specifically, nocturnal telescopes begin operation somewhere

* Email: jeff.shaddix@numerica.us, Phone: 970-207-2200

between -6° and -18° solar elevation (between civil and astronomical dusk) and likewise cease operation between astronomical and civil dawn. This shortened period is exacerbated by the fact that passive optical systems require RSOs to be illuminated, and at such low altitudes most LEO RSOs are regularly behind Earth's shadow during the prime viewing hours of the night. This is not a problem at higher RSO altitudes, such as GEO (∼36,000 km), where the angular extent of the Earth is small enough to rarely cast a shadow (though this does happen for short periods at the vernal and autumnal equinoxes). Thus, in order for nocturnal telescopes to observe a LEO RSO, the observer must be within Earth's shadow, but the object of interest must be outside Earth's shadow. Consequently, nocturnal telescopes have only brief windows after dusk and before dawn during which to observe LEO RSOs. Clearly this is not ideal, and it significantly reduces the utility and cost efficiency nocturnal telescopes can provide towards time-critical LEO SDA.

To further exemplify the issue, there are some sun-synchronous orbits (roughly polar orbits that precess in-sync with Earth's annual revolution) that are at times significantly challenging for any nocturnal telescope system to observe. For instance, the European Space Agency Aeolus satellite uses a 320 km altitude dawn/dusk sun-synchronous orbit, meaning it approximately rides around the day/night terminator. Its orbit tilts with respect to the terminator throughout the year, and there are periods of time when it rides the terminator so closely that existing nocturnal telescope networks struggle to observe it. The opposite sun-synchronous orbit, a noon/midnight orbit, runs perpendicular to the terminator and also poses a challenge. These orbits enter and leave night conditions near the poles while briefly remaining out of Earth's shadow. High latitude sites are necessary to routinely observe these orbits during their small windows of nighttime observability.

So how then can one make ground-based optical telescopes more effective for time-critical SDA? By removing the nocturnal limitation. If an optical system could operate and track LEO RSOs during daylight conditions, then, as will be explored, viewing opportunities increase drastically. To continue the "nocturnal" analogy, optical systems that operate 24/7 can be considered "cathemeral" (active in both day and night conditions). A cathemeral ground-based optical telescope (henceforth dubbed a cathemeral telescope) can, in addition to the nocturnal windows, monitor LEO RSOs throughout daylight conditions when objects are illuminated by both the sun and earthshine. Earthshine, the upwelling radiance from the illuminated Earth reflecting back off the satellite, dominates the signal energy at high solar phase angles. To explore the benefits of cathemeral telescopes, we assess viewability windows from a hypothetical 16-site network. See Sec. 3.1 for more detail on site selection.

To begin, let us reconsider the sun-synchronous dawn/dusk and noon/midnight orbits. Fig. 1a visualizes the orbits for the Oceansat-2 and CHEOPS LEO payloads. Over a 7-day period centered around April 7, 2021, the figure displays the number of observable passes assuming nocturnal (night-only) or cathemeral (day+night) telescopes. As can be seen, moving to cathemeral telescopes increases observable passes by 1800% for the dawn/dusk orbit and 568% for the noon/midnight orbit. Similarly, for an assortment of 250 payloads and rocket bodies, Fig. 1b provides histograms detailing the difference in number of observable passes, and Fig. 2 details the percentage increase with respect to each object. While dependent on orbit, the average increase in observable passes is roughly 400% (or 5x the nocturnal value). This increase in efficiency improves the value proposition for a network of cathemeral optical systems to supplement radar with time-critical SDA. See Sec. 3.2 for a description of how these 250 RSOs were selected and used in later analyses.

In this paper we will further analyze the benefits and drawbacks of a cathemeral telescope network (CTN). But first, we will explore Numerica's currently fielded cathemeral telescope system - "Aquila".

2. RECENT ADVANCEMENTS IN DAYTIME OPTICAL TRACKING

In 2018, Numerica designed and prototyped a daytime-capable optical tracking system named "Aquila" (see Fig. 3). At first this system was limited to tracking RSOs in and near GEO, but in 2020 the technology was successfully expanded to enable daytime tracking of LEO RSOs. At the time of writing, four Aquila systems have been fielded across United States, Australia, and Spain. By the end of 2021, two more systems will be fielded, at least one of which will be outside the contiguous United States.

Aquila uses a combination of customized optics, high speed shortwave infrared (SWIR) cameras, and advanced algorithms to cut through the noise of the daytime sky. The optical chain uses (i) a custom baffle designed to shade the full optical tube from direct sunlight (at solar distance angles above 15°); (ii) a half-meter catadioptric

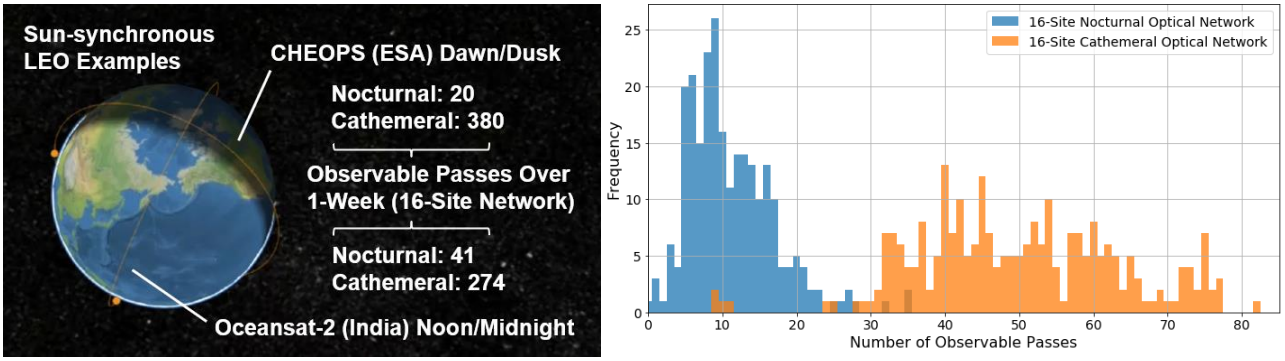

Figure 1. (a) Visualization of dawn/dusk and noon/midnight sun-synchronous orbits and a comparison of the number of observable passes from a 16-site optical telescope network of cathemeral versus nocturnal systems. (b) Similar comparison of the number of observable passes from 250 random LEO payloads and rocket bodies.

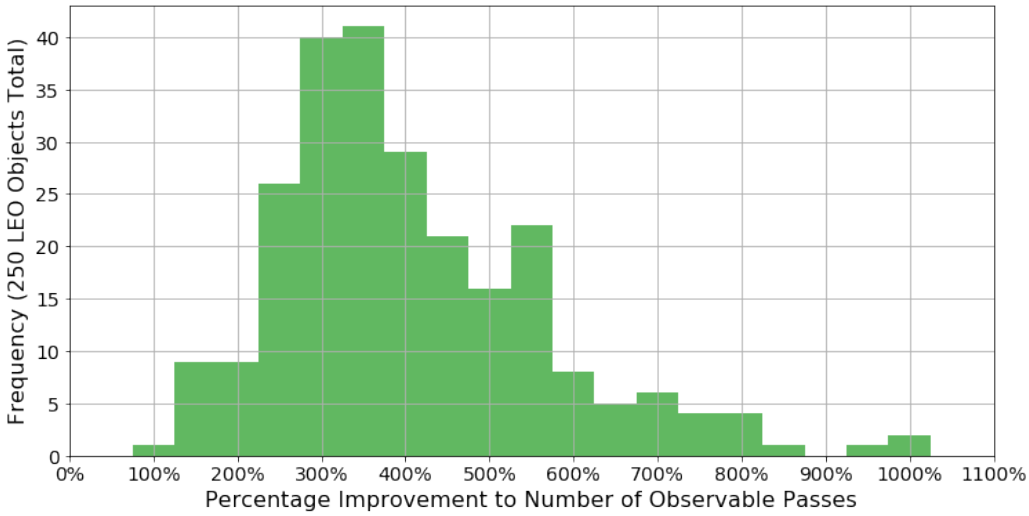

Figure 2. Percentage increase in the number of observable passes on 250 random LEO payloads and rocket bodies between cathemeral telescopes and nocturnal telescopes in a hypothetical 16-site network.

telescope coated to transmit effectively at SWIR wavelengths; and (iii) a custom multi-band filter to optimize detectability and photometry. Aquila's camera operates at hundreds of frames per second to maintain full duty-cycle operation in daylight conditions, producing around 15 GB of data per 60-second GEO observation. This data is consumed by near real-time algorithms that reduce the large data volume, remove multiple sources of noise (correlated and uncorrelated), and produce observations on stars and RSOs. Please refer to our 2019 AMOS paper for Aquila design philosophies and a deeper look into how SWIR sensing is beneficial against a daytime sky background [1].

From June 2020 to August 2021, the Aquila systems have produced over 75,000 daytime observations (sun elevation higher than civil dawn/dusk) on more than 500 unique RSOs spanning high-altitude GEOs (∼36,000 km) to low-altitude LEOs (<500 km). Fig. 4 plots each unique RSO by orbit apogee and maximum detected solar elevation. As can be seen, the Aquila systems have detected a wide assortment of RSOs, even at high solar elevations when background shot noise is at its highest. This is especially true for LEO objects that provide significantly brighter signals than those in MEO and GEO.

Aquila photometry is best defined in the custom SWIR passband of the optical system. This passband, dubbed "YJH magnitude," combines three individual transmission windows around the Y, J, and H spectral bands. For an RSO with spectrally flat reflectivity, YJH magnitudes are approximately 1 magnitude lower than visual magnitudes. This difference originates from the magnitude scale calibration to the star Vega, a hotter

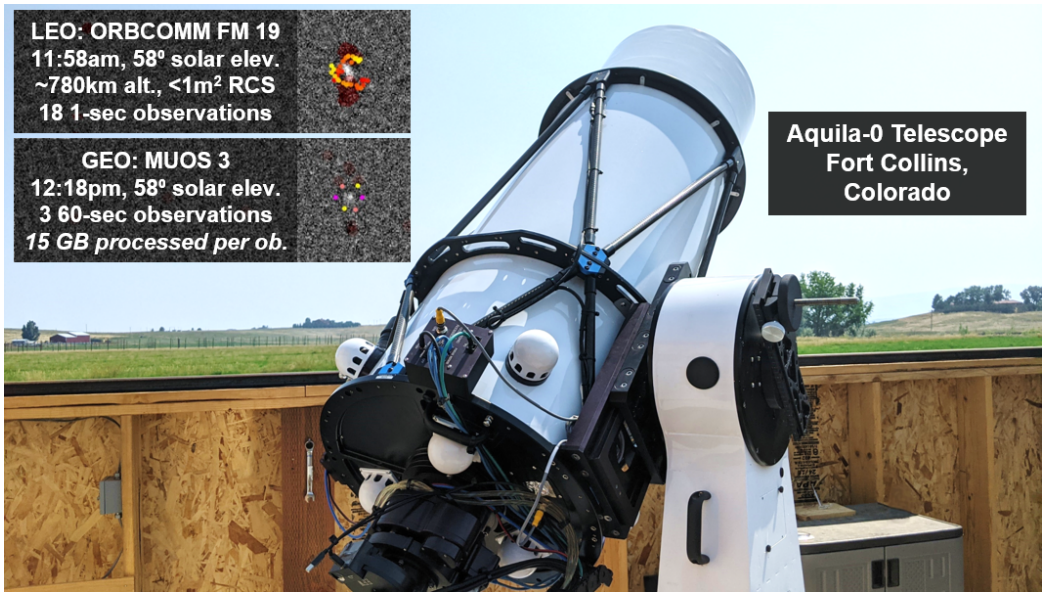

Figure 3. Aquila half-meter cathemeral telescope system and example observations of LEO and GEO satellites at local solar noon. The images are derived from stacking all frames from the collection dwell and overlaying detections with pairs of colored dots in a circular pattern.

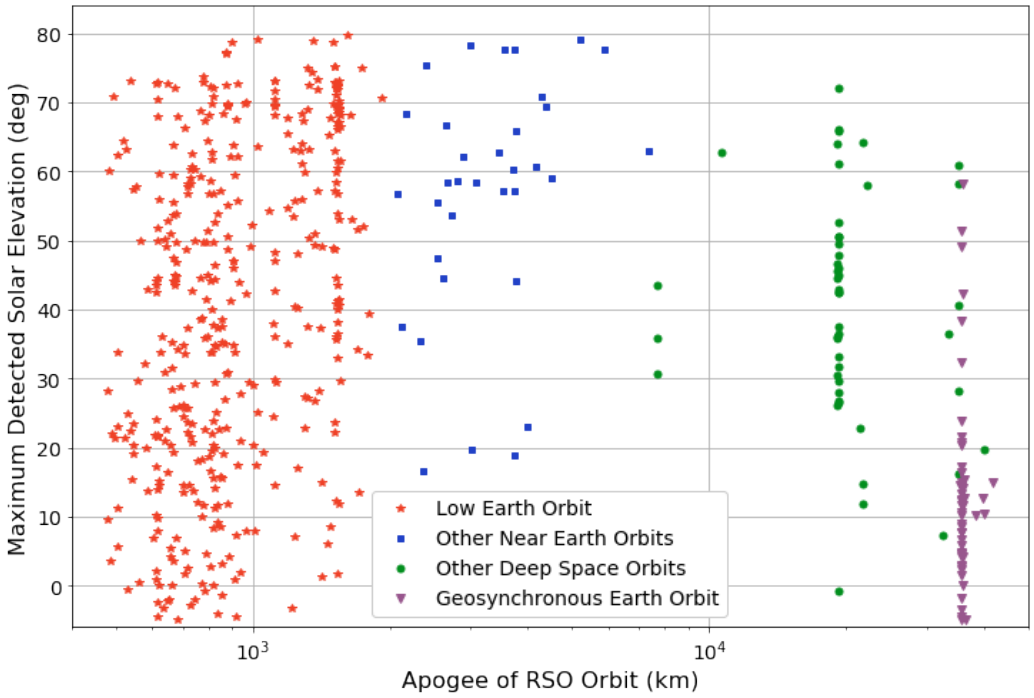

Figure 4. Maximum detected solar elevation for unique RSOs across a 14-month span of cathemeral telescope operations.

black body source than our sun (the RSO illuminator). But RSOs are not spectrally congruent reflectors - characterization efforts of space objects have provided evidence that satellites exhibit higher reflectivity in the near-infrared (NIR) to SWIR regime, particularly around 1.1 um [2]. This drives the difference between YJH magnitude and visual magnitude further. In practice, Numerica has seen an approximate $m_v - m_{yjh} \approx 2$ color magnitude difference when comparing visual and SWIR observations. Fig. 5 provides an example SWIR light curve of the GEO object 'USA 169' (NORAD ID 27711). As seen in this curve, the Aquila daytime detectability

limit on deep space objects is approximately 11.5 m_{yjh} (roughly 13.5 m_v). For objects in LEO, Aquila uses a shorter 1-second observation cadence, lowering the detection limit to approximately 9 m_{yjh} (roughly 11 m_v). At night, these detection limits improve by up to 4 magnitudes.

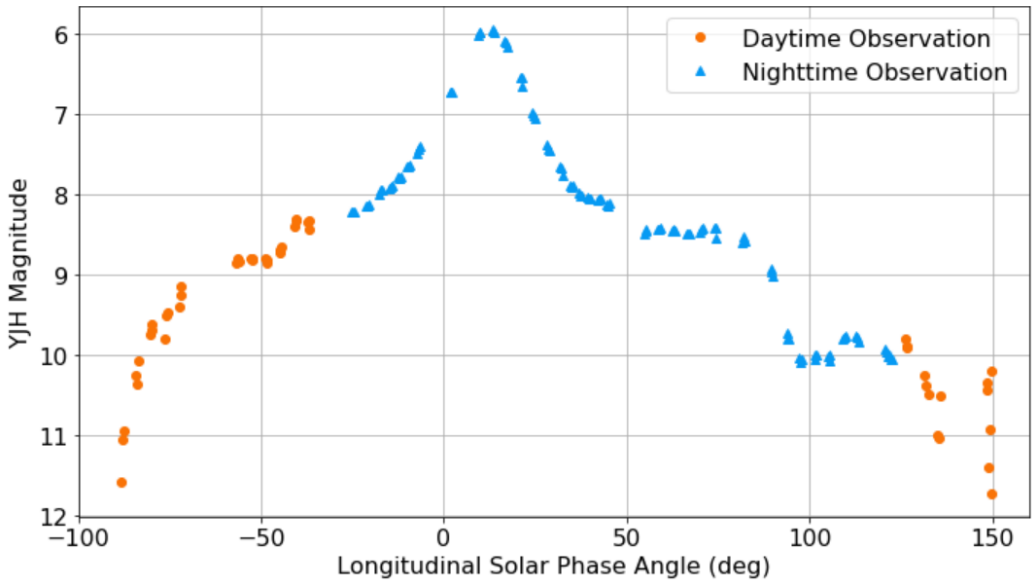

Figure 5. YJH-band photometric light curve on GEO object USA 169 between April 7-8, 2021.

In June 2021, Numerica studied the accuracy of Aquila observations by comparing RSO measurements against interpolated states published by the International Laser Ranging Service (ILRS), see Fig. 6. This service publishes regular, high-accuracy ephemerides on satellites in multiple regimes[†]. The errors from Aquila were split into in-track (along the angular velocity vector) and cross-track (cross product of the in-track direction and line-of-sight). For low angular tracking rates (deep space), Aquila accuracies were measured to be below 4 arcseconds root-mean-squared (RMS). Likewise for high angular tracking rates (LEO), Aquila accuracies were measured to be less than 10 arcseconds RMS. In both cases the errors are composed of a dominant bias component that changes per collection, and a smaller residual component of around 1 arcsecond. While these biases might not be as good as some nocturnal telescope systems, Aquila does not often get in-situ stars to perform attitude correction. Instead, Aquila uses a high-accuracy pointing model combined with regular star collections throughout the day to keep the model accurate. These updates mitigate errors associated with the nychthemeral thermal expansion and contraction cycles in the optomechanical components. Numerica expects these accuracies to continue to improve as the technology matures.

3. SIMULATING HYPOTHETICAL NETWORKS AND THEIR CONSTRAINTS

To assess the benefits offered by cathemeral telescopes to enhancing timely LEO SDA, we simulated a hypothetical 16-site cathemeral telescope network (CTN) subject to constraints imposed by simulated site locations, real-world LEO object populations, and system performance metrics informed by Numerica's existing cathemeral systems. As will be analyzed in Sec. 4, sixteen sites were chosen as a baseline to provide roughly one-hour revisit rate performance when tracking 250 RSOs. Wherever possible, we used real-world data to formulate these constraints, and are therefore confident they present a realistic model of cathemeral telescope performance.

To evaluate cathemeral optical as an augmentation to existing radar capabilities that dominate LEO SDA, we also simulated a 4-site radar network based loosely on LeoLabs' real-world sensor deployments and publicly-available revisit and accuracy statistics as of early 2021. To be clear, we are not suggesting the performance simulated here would be indicative of the LeoLabs radar network. Since Numerica does not own or operate radar

[†]https://ilrs.gsfc.nasa.gov/

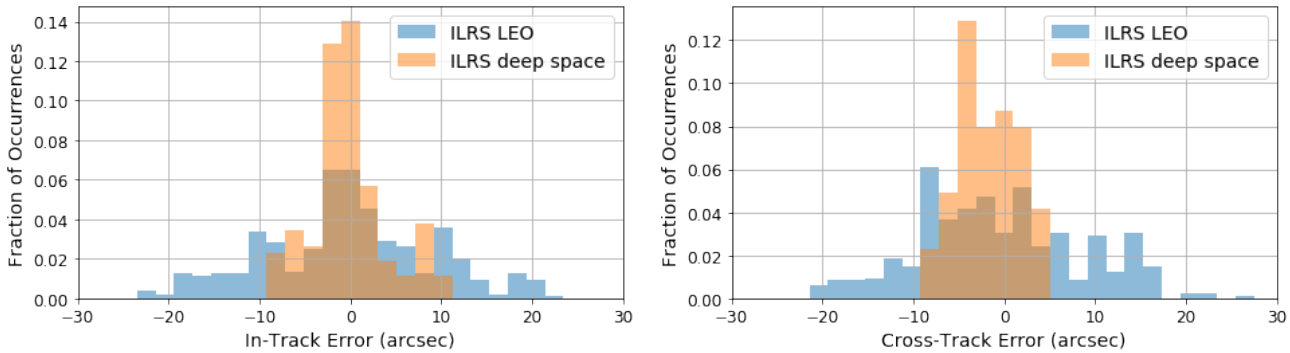

Figure 6. Aquila observation in-track and cross-track error distribution measured against high-accuracy ephemerides published by ILRS. 471 and 129 samples were used for the LEO and deep space distributions, respectively.

systems for SDA, we do not wish to make unsubstantiated claims about the performance of such systems. We are therefore intentionally optimistic about the constraints we impose on simulated radars wherever quantitative information is not publicly-available (see Sec. 3.1). By simulating the performance of these networks together and in isolation, we show the efficacy of low-cost cathemeral optical as an augmentation to high-cost, high-capability radar networks. We describe here site locations, system constraints, and simulation methodology used in the present study.

3.1 Site Locations and System Constraints

For any ground-based sensor performing SDA tasks, site location is a crucial constraint on system utility, as it determines, at minimum, when and where a given RSO's orbit is accessible from the system. Relevant to optical systems, site location also determines weather, which further constrains viewing opportunities. Our simulated 16-site CTN locations are therefore chosen for high geographic diversity, spanning equatorial to polar latitudes globally, and clear weather, with each site subject to mean annual afternoon cloud cover of 35% or less as determined by NASA MODIS Cloud Mask data [3]. Our simulated 4-site radar network, meanwhile, uses the real-world locations of LeoLabs' four radar sites as of June 2021. Simulated sites are shown in Fig. 7.

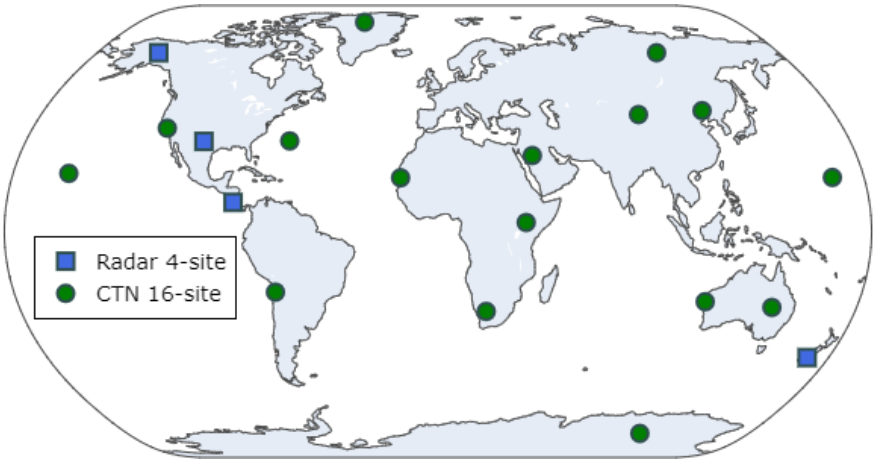

Figure 7. Hypothetical sensor laydown for simulation: sixteen cathemeral telescope sites and four radar sites.

We modeled several important technical constraints of cathemeral telescope systems that determine whether or not a given object in the sky is actually observable. These constraints include weather outages, horizon limits, detectability limits, solar exclusion, duration of satellite pass, and the limitations of rate tracking. We used a simple, binary weather model in which a given site is either "weathered out:" unable to produce observations, or "weather free:" able to produce observations so long as other constraints are satisfied. Every three hours of

simulations time, each site's weather status was determined randomly and independently to be "weathered out" with probability 0.35 or "weather free" otherwise. This weather model is a crude approximation for what is, in reality, a complicated random process, but is nonetheless a model we consider reasonable enough to account for weather outages given our widely-spaced site locations and the high-level metrics of network performance we present in later sections. A fixed horizon limit of 20° elevation was chosen for all sites and applied such that objects below the horizon limit are never observable and objects above the horizon limit are observable if all other constraints are met. This value was chosen to mitigate challenges such as poor atmospheric seeing, distant clouds, and direct obscuration by landscape features. Detectability limits were chosen to be 11 m_v in daytime conditions and 15 m_v otherwise, where a given site was considered in "daytime" if the Sun was fewer than 12° below the horizon, i.e. between nautical dawn and nautical dusk. This constraint was again applied as a binary constraint, such that objects dimmer than the detectability limit are unobservable, and objects brighter are observable only if other constraints are satisfied. In reality, detectability limits vary smoothly with time of day, sun angle, and several other factors, but this simple model captures the majority of detectability variation experienced by real-world cathemeral systems deployed by Numerica. Solar exclusion was applied as another binary constraint, with no object observable fewer than 20° from the sun but otherwise viewable subject to other constraints. The narrow FOV of existing cathemeral telescope systems makes serendipitous collects (observations on a nearby, but un-tasked object) unlikely when observing LEO. We therefore ignore serendipitous collections in our simulations, constraining each telescope to view only one object during a given collection period.

Constraints for simulated radars were substantially more relaxed. Radar systems were simulated as able to view all objects in the sky above 20° elevation angle simultaneously (an overly optimistic assumption) and were modeled as having a probability of detection of 100% (an overly optimistic assumption), regardless of object size or orbit. Radar system uptime was also modeled as 100% (an overly optimistic assumption).

3.2 Simulated LEO Catalog

We chose 250 real-world LEO objects to test performance of the simulated sensor networks. The set of objects chosen was meant to capture the diversity of the non-debris LEO object population as of June 2021. To compute viewing geometries and access times, the latest publicly-available SpaceTrack.org state as of June 14, 2021 was used for each object and propagated as needed. Network performance was simulated on these objects for the 7-day period beginning on June 14, 2021, 19:37 UTC. Where needed to compute cathemeral telescope viewing constraints, photometry for each object was modeled using a spherical body and rectangular solar-panel model derived from prior work by Rita Cognion [4] and Jovan Skuljan [5]. The parameters in this model were calibrated using real-world Numerica Telescope Network observations and a per-object scale factor determined using publicly available radar cross section values from CelesTrak[‡]. This is a crude photometry model for any given object, but one we have found effective at modeling bulk statistics computed over populations of RSOs.

3.3 Simulated Tasking and Collection

To simulate coordination and tasking of multiple sensors on multiple objects, we implemented a simple "greedy" scheduler. We first discretized the simulated 7-day period into one-minute planning periods. For each planning period, the scheduler iterated through all sensors considered, computing for each sensor objects visible for at least six seconds during the planning period, where visibility was determined by an object successfully meeting either the set of cathemeral telescope constraints or radar constraints previously mentioned (appropriate for the sensor considered). The planner would assign each telescope the oldest (longest time since last update) object available to that telescope, while proactively storing an update time for that object equivalent to the start of the planning window (to prevent the next sensor scheduled from visiting the same object during the current planning window)[§]

Radar systems, on the other hand, were assigned all objects visible during the planning window, with a proactive update time stored for each. Joint scheduling of radars and cathemeral telescopes was meant to

[‡]https://celestrak.com/

[§]We remark that more optimal sensor tasking is indeed possible, but incorporation of such tasking is beyond the scope of the present study.

simulate a hypothetical collaboration between network operators. These networks were also simulated in isolation for comparison.

Although not strictly necessary, we have found it desirable to perform extensive self-calibration routines on cathemeral telescopes prior to collecting on a given LEO object. This increases probability of capturing the RSO within the FOV as well as the overall observation accuracy. To account for this self-calibration period, we made each telescope unavailable for scheduling for two out of every three planning periods. This reduces the overall cathemeral telescope capacity, but ensures plenty of overhead for producing high quality data for timely LEO SDA needs. Numerica is presently investigating techniques to reduce this calibration time in its fielded systems.

When assigned to a given object for a planning period, a cathemeral telescope is simulated to collect one-second observations for the duration of the pass visible during the planning window. If the pass does not take up the whole planning window, the telescope will wait (this would be inefficient in reality, but substantially simplifies our simulated planning). Each cathemeral telescope observation is simulated as a line-of-sight angle/angle measurement from observer to RSO position with addition of a random noise and bias. The bias value for a simulated right-ascension/declination (Ra/Dec) observation is drawn randomly per pass from a two-dimensional Gaussian random vector with zero-mean and a diagonal covariance matrix $\Sigma_{\text{bias}} = \text{diag}(\sigma^2_{\text{ra-bias}}, \sigma^2_{\text{dec-bias}})$, where $\sigma_{\text{ra-bias}} = \sigma_{\text{dec-bias}} = 8.5$ arcseconds, while the noise value is drawn randomly per observation from a two-dimensional Gaussian random vector with zero-mean and a diagonal covariance matrix $\Sigma_{\text{noise}} = \text{diag}(\sigma^2_{\text{ra-noise}}, \sigma^2_{\text{dec-noise}})$, where $\sigma_{\text{ra-noise}} = \sigma_{\text{dec-noise}} = 1.5$ arcseconds. These noise (sigma) values are based on data collected from real-world cathemeral telescope systems. Radars, assigned to collect on all visible objects during all planning periods, are simulated to collect 20 observations per visible object per radar per pass, with observations over a pass spaced uniformly in time. Simulated radar observations were subject to zero-bias and a noise value drawn randomly per observation from a two-dimensional Gaussian random vector with zero-mean and a diagonal covariance matrix $\Sigma_{\text{noise}} = \text{diag}(\sigma^2_{\text{range-noise}}, \sigma^2_{\text{doppler-noise}})$, where $\sigma_{\text{range-noise}}$ was chosen to be 18.0 meters, and $\sigma_{\text{doppler-noise}}$ was chosen to be 0.18 m/s. The simulated observation cadence and measurement accuracy were consistent with sensor-level and network-level statistics made publicly-available by LeoLabs [6].

4. CTN AUGMENTATION IMPACT TO OBSERVATION TIMELINESS

In this section we explore the impact of CTN site quantity on RSO time since last observation (TSLO). This TSLO metric is distinct from a gap time metric, but we believe it is more appropriate for timely SDA requirements. Gap times measure the delays between subsequent observations, whereas TSLO measures the amount of time since last observation *from a uniformly sampled set of times over an extended period*. TSLO provides a metric to provide statistical analysis against the question "how long has it been since we have seen the object?" where that question could be raised at any point in time on objects under surveillance custody.

We begin by exploring the TSLO trade space when varying the number of deployed cathemeral telescope sites and the number of objects on which to maintain custody. Fig. 8 explores this space by plotting the average TSLO for a 4-site, 8-site, and 16-site CTN as a function of objects maintained. The 4-site radar network average TSLO is also provided for comparison.

For lower tasking demands, each optical system is typically able to service all potential collections (other constraints permitting). As such, an 8-site CTN provides roughly equivalent mean TSLO performance against a 4-site radar network at around 50-100 objects in custody. Weather outages and times when RSOs fall in Earth's shadow explain the need for the additional CTN sites to match TSLO performance. For higher tasking demands, optical systems may need to choose between conflicting RSO collection opportunities. For this simulation, tasking priority was set through sorting the objects by age of last state update. Thus, at 200-250 objects in custody, the mean TSLO for an 8-site CTN diverges higher than the 4-site radar network as capacity limitations take effect. This highlights the efficacy of radar systems for bulk RSO tracking and reinforces that cathemeral telescope systems should be used on a critical subset of the LEO population to meet timely SDA requirements. For the remainder of this paper we will focus on a 16-site CTN, selected to achieve an approximate 1-hour average TSLO when tasking against a set of 250 RSOs.

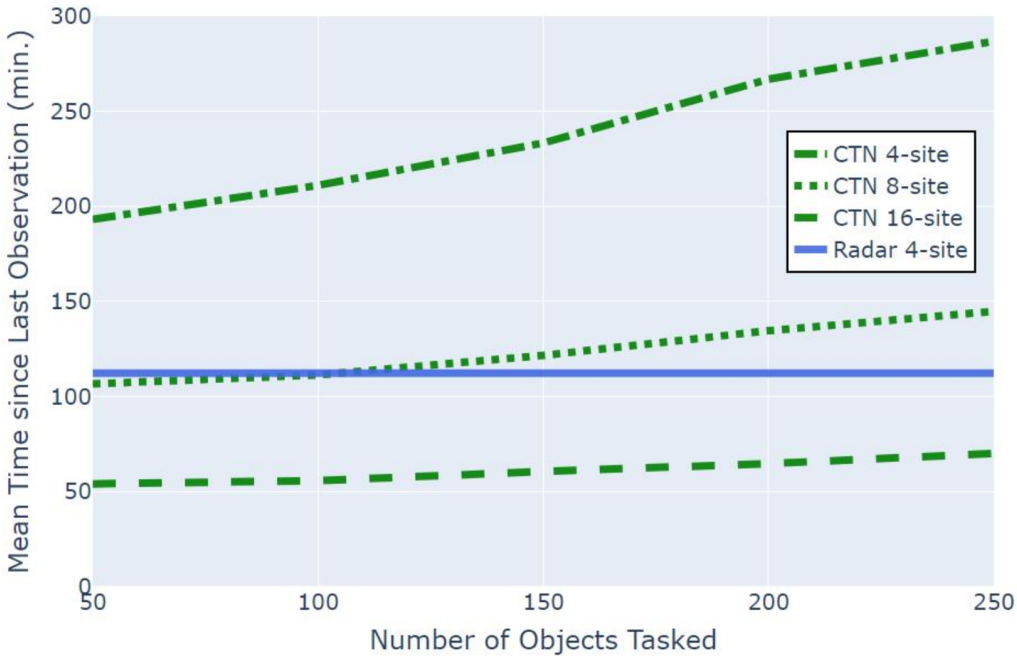

Figure 8. Comparison of independent network custody performance by number of cathemeral optical sites and number of LEO RSOs maintained. Performance from a simulated 4-site radar network is shown for comparison.

We now consider the distributions of TSLO from a 16-site CTN, 4-site radar network, and the fusion of both networks (20 sites total). Fig. 9 provides cumulative distribution functions (CDFs) on the TSLO metric against our 250 LEO RSO set from each network configuration. The distribution means/medians from these options are, in minutes: 112/66 (radar network), 68/49 (CTN), and 41/29 (joint network). Here the typical (median) case is close between the radar network and the CTN, but the radar network has a more prominent tail skewing the means. The fusion of these networks provided a significant improvement over each independent network.

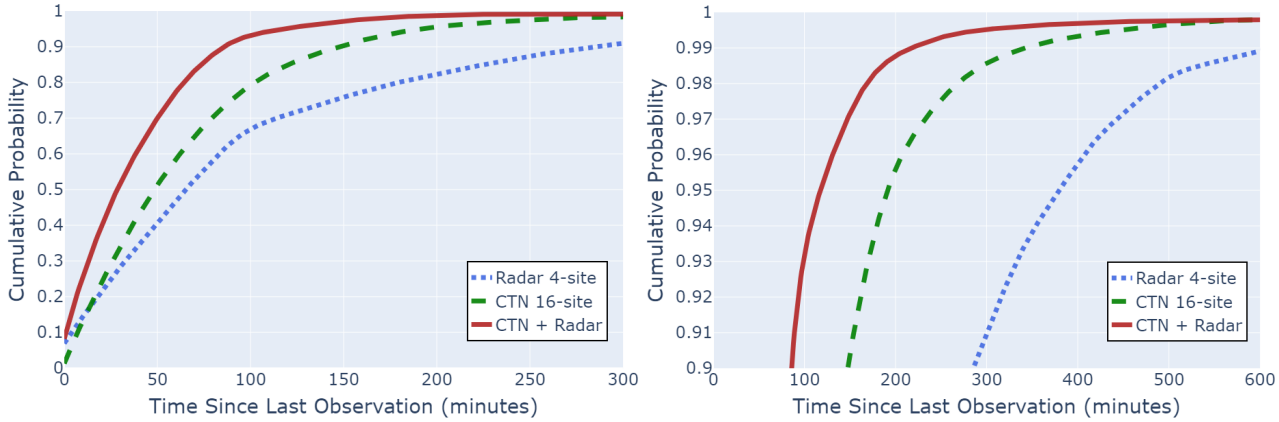

Figure 9. Cumulative distribution function of times since last observation across a set of 250 LEO RSOs. Plot on right is scaled to show detail above the 90th percentile.

While monitoring 250 objects may be useful for nominal operations, there may be times when priorities shift towards critical monitoring of an even smaller set of RSOs. Thus, we explore the 16-site CTN benefits towards maintaining custody of a set of 1-50 objects. This helps determine the maximum benefit of the 16-site CTN when the risk of overlapping RSO passes at a specific site is low. Fig. 10 shows the results of a Monte Carlo

simulation where random subsets of the 250 RSO base set are passed through the same viewability calculation as described in Sec. 3.3. The mean and 1-sigma error bounds are presented to get a sense for the distribution and dependence on specific orbits. The radar network continued its average 110 minute mean TSLO as expected. The CTN increased from a 40 to 50 minute mean TSLO as the number of objects increased from 1-50, whereas the fusion of these networks again outperform the parts, providing a near constant 33 minute mean TSLO. Thus, a joint network could provide on average half-hour TSLO for a critical subset of objects.

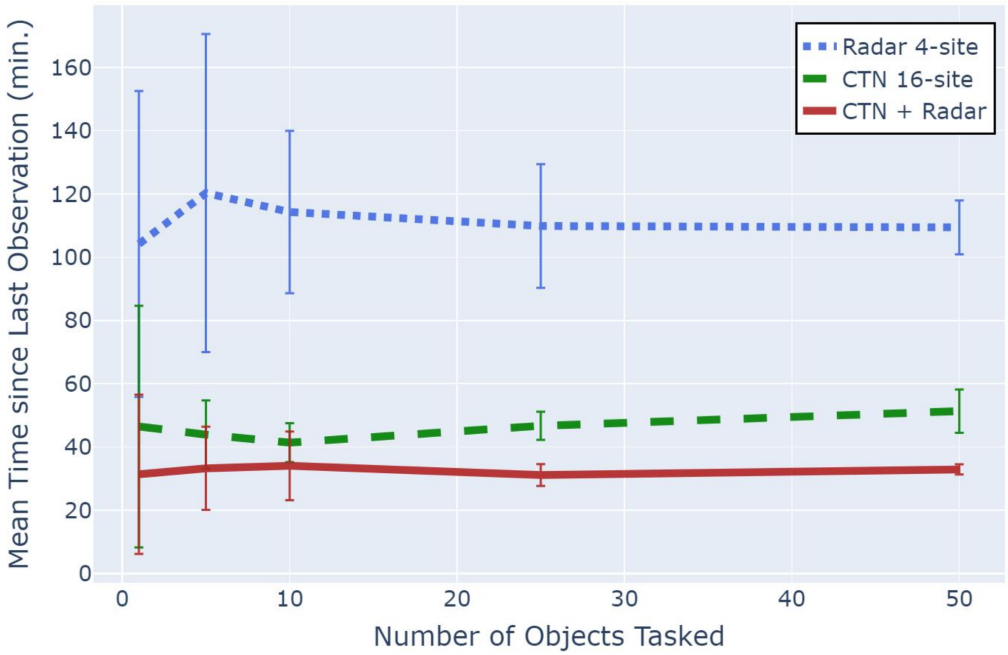

Figure 10. Monte Carlo simulation showing the mean time since last observation on various LEO RSO set sizes. Error bars represent the upper and lower 1-sigma error bound.

5. CTN AUGMENTATION IMPACT TO ORBITAL STATE ACCURACY

More frequent observations do not guarantee significant improvement to orbital state accuracy, especially in the case of quiescent RSOs. For example, if observation accuracy is poor and the RSO orbit fits the expected propagation model, additional measurements may not be able to provide novel information to the tracking system. In contrast, for cases where the RSO orbit is not quiescent (e.g. from a maneuver), even low-accuracy measurements may provide enough information to significantly improve state accuracy. In this section we study the former case, verifying that lower TSLO values translate into increased orbital state accuracy even on a quiescent RSO.

We begin by taking simulated observations against the truth ephemerides of KOMPSAT-5, a South Korean ILRS satellite in dusk-dawn orbit at 550 km altitude. These observations are run through an unscented Kalman filter (UKF) [7] which fuses the range/doppler and angle/angle measurements from radar and optical systems to produce state mean and covariance information over a week-long simulation period. We use a high-fidelity orbital propagator for state transition (32-order gravity model) and have tuned the process noise to give near ideal Mahalanobis distances in our state covariances. This process noise is non-isotropic due to drag dominating the uncertainty. We used 1e-5 radial, 5e-5 in-track, and 2e-5 cross-track (all in m/s^2) to initialize this process noise in all three network configurations. Further tuning of this process noise could have been performed, though in practice an ideal process noise is dependent on characteristics of each RSO.

Similar to the TSLO metric used before, we measure tracking position error at randomly distributed time points during the simulation. This gets to the question "how well do I know where the object is right now?"

where that question could be raised at any point in time on objects under surveillance custody. Unlike TSLO, the results are shown only for the final three days of the week-long simulation. This allows us to focus on steady state tracking performance when state covariance has stabilized from any startup transients (e.g. from use of two-line element set in creating the initial state estimate). Further study could be performed to analyze variation in tracking error over time since a custody requirement was generated, though this will be dependent on a-priori orbit state accuracy and other factors.

Fig. 11 provides the output of this simulation, displaying the tracking position error as distance from truth ephemerides. As expected, this error rises the longer KOMPSAT-5 goes unseen, then snaps back to lower error upon receiving measurements. This effect is more pronounced on the radar scenario given the 4-site vs 16-site difference in geographic diversity. A CDF of normalized Mahalanobis distances is also provided to show that the UKF is appropriately sizing its state covariance (uncertainty) through proper use of process and measurement noise estimates.

Fig. 12 provides CDFs of the tracking position error across the steady state period of the simulation. These plots clearly show the benefit a CTN can provide toward reducing position uncertainty. The position error averages for the three cases were 34.4 m for the 4-site radar network, 25.2 m for the 16-site CTN, and 18.7 m for the fused network. Thus, the fused network provided an average decrease in tracking position error of 46% and 26% compared to the radar and CTN independent networks, respectively. This improvement amplifies at the higher percentiles of the CDF where confidence requirements are typically generated.

While this example provides some confidence in the tracking benefits of a CTN, as mentioned earlier, a more compelling use case would be against a less quiescent object. If a LEO RSO maneuvers during the custody period, the higher revisit rate of the CTN would be able to more quickly reacquire the object and subsequently correct its orbital state estimate. Further analysis would be needed to quantify these benefits.

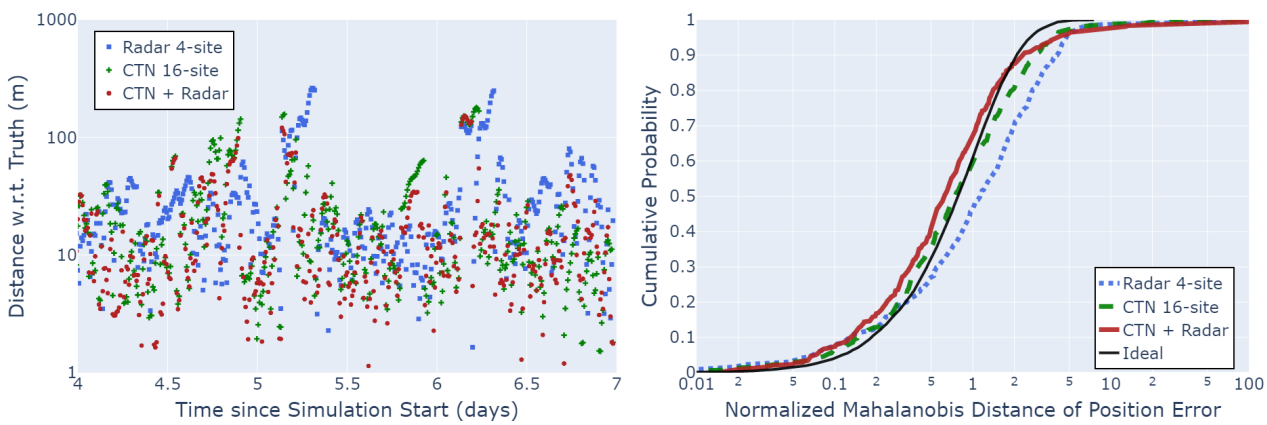

Figure 11. (a) Tracking position error time profile against ILRS object KOMPSAT-5 over the last 3 days of the 7-day simulation period. (b) Cumulative distribution function of the Mahalanobis distances from state position error (normalized for 3-dimensional position).

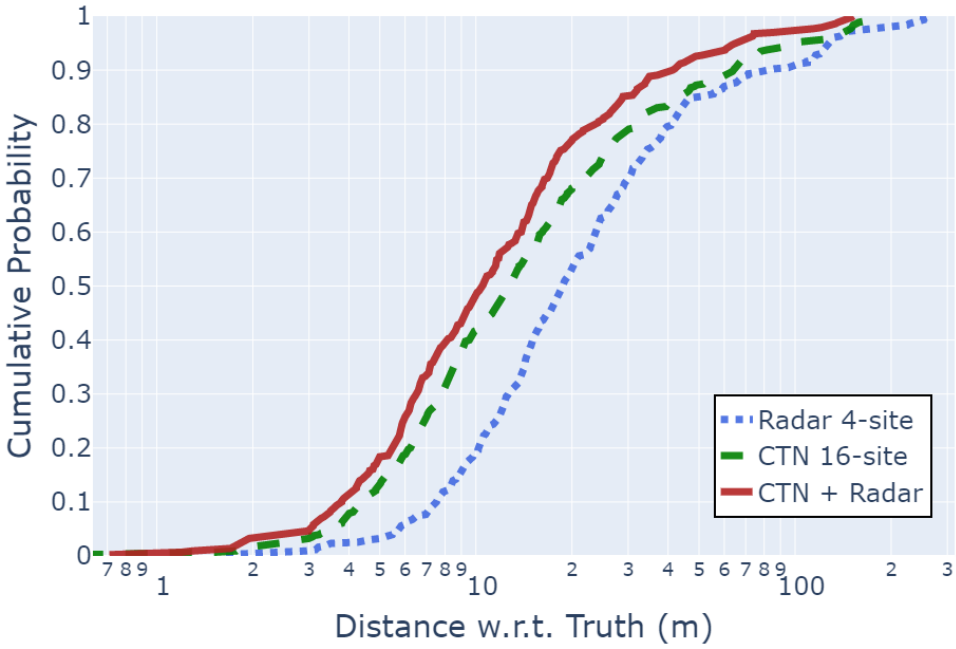

Figure 12. Cumulative distribution function of tracking position error over the last 3 days of the 7-day simulation period.

6. CONCLUSIONS

Through this paper we have discussed the need for timely SDA in the LEO regime, the benefits of daytime observation of LEO RSOs, the characteristics of Numerica's daytime-capable Aquila system, and the simulation results of a cathemeral telescope network working in concert with a radar network. The latter results point to the significant improvements in timely SDA against a random subset of payloads and rocket bodies in the LEO population. Specifically, by fusing a 16-site cathemeral telescope network with a 4-site radar network, our simulations suggest significant reductions in both "time since last observation" and tracking state position error metrics.

While these improvements point to the utility of a cathemeral small aperture telescope network, we want to remind the reader that radar systems and optical systems are complementary. Radar systems are better suited for tracking RSOs in LEO when high revisit rates are not necessary (e.g., for bulk catalog maintenance). Likewise, large-aperture optical telescopes such as are used in the Ground-based Electro-Optical Deep Space Surveillance (GEODSS) program are needed to track dim objects that smaller aperture optics simply cannot detect. Other phenomenologies such as passive radio frequency and space-based optical also have important roles in fulfilling the SDA mission. The breadth of needs and applications within SDA necessitates the use of multiple tools to solve its challenging problems. Nevertheless, for timely SDA on a subset of LEO RSOs, we conclude that a cathemeral telescope network may be just the right approach.

ACKNOWLEDGMENTS

We acknowledge and appreciate support from U.S. Space Force, Air Force Research Laboratories, and Numerica's internal research and development program.

DISTRIBUTION

Cleared for Public Release (Case Number PA-2471, 2 September 2021).

REFERENCES

[1] J. Shaddix, J. Brannum, A. Ferris, A. Hariri, A. Larson, T. Mancini, and J. Aristoff, "Daytime GEO tracking with aquila: Approach and results from a new ground-based SWIR small telescope system," in *Proceedings of the 2019 Advanced Maui Optical and Space Surveillance Technologies Conference*, (Wailea, HI), September 2019.

[2] K. J. Albercromby, P. Abell, and E. Barker, "Reflectance spectra comparison of orbital debris, intact spacecraft, and intact rocket bodies in the GEO regime," in *Proceedings of the Fifth European Conference on Space Debris*, (Darmstadt, Germany), March 2009.

[3] NASA, "NASA EarthData LAADS DAAC MODIS Cloud Mask." `https://ladsweb.modaps.eosdis.nasa.gov/missions-and-measurements/science-domain/cloud-mask/`. Accessed: May 2021.

[4] R. Cognion, "Observations and modeling of GEO satellites at large phase angles," in *Proceedings of the 2013 Advanced Maui Optical and Space Surveillance Technologies Conference*, (Wailea, HI), September 2013.

[5] J. Skuljan. private communication. Discussion: September 2019.

[6] LeoLabs, "Leolabs system metrics." `https://platform.leolabs.space/system_metrics`. Accessed: June 2021.

[7] S. J. Julier, J. K. Uhlmann, and H. F. Durant-Whyte, "A new method for the nonlinear transformation of means and covariances in filters and estimators," *IEEE Transactions on Automatic Control*, vol. 55, pp. 477–482, 2000.